

Stiffness and atomic-scale friction in superlubricant MoS₂ bilayers

Rui Dong,* Alessandro Lunghi, and Stefano Sanvito

School of Physics, AMBER and CRANN Institute, Trinity College, Dublin 2, Ireland

(Dated: July 2, 2021)

By using *ab-initio*-accurate force fields and molecular dynamics simulations we demonstrate that the layer stiffness has profound effects on the superlubricant state of two-dimensional van der Waals heterostructures. These are engineered to have identical inter-layer sliding energy surfaces, but layers of different rigidity, so that the effects of the stiffness on the microscopic friction in the superlubricant state can be isolated. A twofold increase in the intra-layer stiffness reduces the friction by approximately a factor six. Most importantly, we find two sliding regimes as a function of the sliding velocity. At low velocity the heat generated by the motion is efficiently exchanged between the layers and the friction is independent on whether the sliding layer is softer or harder than the substrate. In contrast, at high velocity the friction heat flux cannot be exchanged fast enough, and the build up of significant temperature gradients between the layers is observed. In this situation the temperature profile depends on whether the slider is softer than the substrate.

When the lateral forces between two sliding surfaces vanish or become extremely small, the surfaces are said to be superlubricant [1], a state often defined by a friction coefficient smaller than 0.01. Structural superlubricity [2] is a particular superlubricant situation that emerges between dry and flat surfaces with incommensurate lattices. This structural peculiarity drastically suppresses the corrugation of the inter-layer sliding energy surface (ISES), so that the relative motion can take place with very limited energy dissipation. The ideal conditions for structural superlubricity are found when: i) the two surfaces are extremely rigid, so that elastic deformation is prevented over long length-scales; and ii) the surface-to-surface interaction is weak [3].

Two-dimensional (2D) materials, such as graphene, h-BN and transition metal dichalcogenides, are characterised by strong in-plane covalent bonds and weak inter-layer van der Waals interaction. Thus, vertically stacked 2D heterostructures appear as an ideal materials platform for structural superlubricity. 2D compounds have been used as solid-state lubricants since many years [4, 5], although only recent advances in atomic-force microscopy have given us a thorough microscopic understanding of the superlubricity phenomenon [6]. One can now find experimental demonstrations of structural superlubricity in graphene [7–10], MoS₂ [11–13], and in heterogeneous structures, h-BN/graphene [14] and WS₂/graphene [15, 16].

Among the possible theoretical strategies to study microscopic tribology [17] the “quasi-static” approach has enjoyed significant popularity. This consists in computing the frictional forces from the gradient of the ISES [18], which in turn can be obtained with *ab-initio* methods. [19] A variation of the same approach monitors the energy and forces during the movement of a “slider” over a “substrate”, when the layers’ internal degrees of freedom are either kept frozen [20, 21] or allowed to relax [22].

This is a good solution when looking at effects involving extended defects, such as grain boundaries, which require large simulation cells [23]. In general, the quasi-static approach works well in systems where the ISES is deep and the friction is dominated by the slider center of mass (CM) scattering. However, in a superlubricant situation the external forces dissipate into the internal atomic motion, a process that requires a molecular dynamics (MD) approach. In this case the most typical setup consists in attaching the slider to a moving support through harmonic springs and in monitoring the spring forces over the MD trajectories [24–26]. Empirical force fields are usually employed in this approach.

Here we use highly accurate machine-learning force fields, together with MD simulations without external driving forces, to answer a simple but crucial question: does the stiffness of the sliding layer affect the friction of a superlubricant system? We find that indeed this is the case, a twofold increase in the intra-layer stiffness reduces the friction by approximately a factor six. Most importantly, the stiffness mismatch between the slider and the substrate determines the thermal coupling between layers and the heat dispersion dynamics, resulting in different friction regimes at different sliding velocities.

Our simulations are for MoS₂ bilayers. The in-plane forces are described by a spectral neighbor analysis potential (SNAP) [27], generated with a procedure described before [28]. This delivers a total-energy accuracy of 1.8 meV/atom, namely the MoS₂ potential energy surface is almost identical to the density-functional-theory (DFT) one, which is used to fit the SNAP. A simple Lennard-Jones potential extracted from van der Waals DFT calculations [29] is employed for the inter-layer interaction. This returns a bilayer binding energy of 32.1 eV/Å² for the 2H order, which is close to that computed by DFT, 35.7 eV/Å². Similar results are obtained for other bilayer polymorphs. In addition, we generate two more SNAPs, obtained by rescaling the total energy of the distorted configurations included in the training set by either a factor 2 or a factor 1/2 (the total energy is measured from that of the equilibrium configu-

* Contact email address: dongru@tcd.ie

ration). The resulting potentials have all the same energy minimum, namely the MoS₂ equilibrium geometry, but simulates materials with different stiffness (re-scaling the forces by a factor α changes the elastic tensor by the same amount). Layers described by these three SNAPs are denoted as *normal* (N), *soft* (S) and *hard* (H), respectively. Importantly, note that any bilayer constructed from these SNAPs has the same ISES. This not only allows us to perform dynamic simulations of friction in real materials with DFT accuracy, but also to isolate the effect of the in-plane stiffness on the superlubricity from those associated to the corrugation of the ISES.

Our elemental structure is a $\sqrt{7} \times \sqrt{7}$ cell, in which the superlubricant state is obtained by applying a twist angle of 21.8° between the two layers from the 2H configuration. This is the smallest strain-free cell that can be constructed [30], returning a ISES corrugation of less than 0.1 meV/Å². The MD simulations are then conducted over a 6×6 supercell of the $\sqrt{7} \times \sqrt{7}$ cell with periodic boundary conditions. One of the layer, the substrate, is kept fixed by removing the linear momentum of its CM at every MD step, while the other, the slider, is set in motion with an initial velocity of $v_0=800$ m/s (see Fig. 1). This rather high initial value (a piston in a combustion engine moves at ~ 25 m/s) gives us a velocity range large enough to converge well the friction-vs-velocity curve. Note that our very flat ISES makes the slider performing Brownian motion at ~ 30 m/s in equilibrium at room temperature. The system is equilibrated at 300 K using a Nosé-Hoover thermostat for 1 ns. After equilibration, snapshots are taken every 0.5 ns and used as the starting point for the sliding. With this set up the slider moves freely on the substrate, while its CM velocity is measured. Note that there is no constraint on any part of the slider, a fact that ensures the internal atomic vibrations not to be altered. During the sliding process the temperature of the substrate is thermostated at 300 K, but the temperature of slider is not controlled. This mimics experiments in vacuum, where the slider can only exchange energy with the substrate. Bilayer types are denoted as α - β ($\alpha, \beta = S, N$ and H) with α (β) defining the slider (substrate). For each configuration multiple MD runs are carried out to reduce the noise, and the analysis will be performed over the averaged trajectories.

Fig. 1 shows the time evolution of the slider CM velocity for the nine possible bilayers. Clearly, the layer stiffness has a significant effect on the friction, since it takes only 2 ns to stop the soft MoS₂ bilayer (from its initial velocity of 800 m/s), while the normal and hard MoS₂ bilayers take ~ 10 ns and ~ 40 ns, respectively. When combining monolayers of different stiffness, the general trend is maintained with the harder combinations preserving the motion for longer times. A minor anomaly appears for the combination with the largest stiffness mismatch between the layers, since the curves for H-S and S-H are not identical. We will come back on this point.

The acceleration-velocity curve, $a(v)$ can be obtained by simple finite-difference differentiation of the $v(t)$ curve

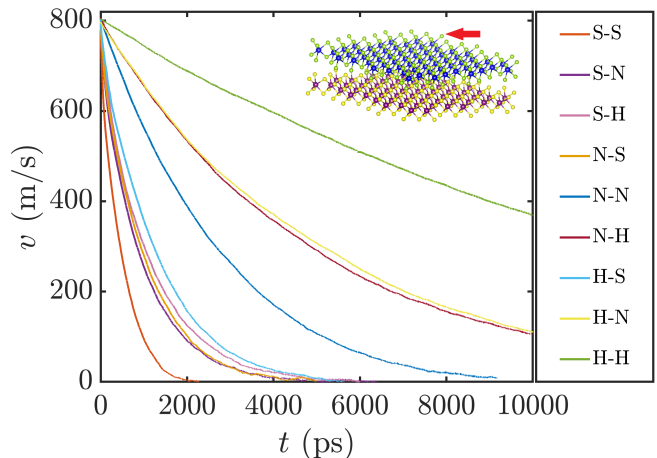


FIG. 1. (Color online) Time evolution of the velocity of the slider center of mass for the 9 bilayer types investigated. Inset: A ball-and-stick representation of the system used in the MD simulations, where a slider MoS₂ monolayer (top) moves above a MoS₂ substrate (bottom). Color code: Mo = blue/purple, S = green/yellow.

over 5 m/s steps. Thus, the frictional force per unit area can be computed as $f(v) = \rho_s a(v)$, with $\rho_s = 18.84$ a.u./Å² being the 2D density of the MoS₂ monolayer. Such quantity is presented in Fig. 2(a) against the slider velocity for the soft (S-S), normal (N-N) and hard (H-H) bilayers. We empirically find that the frictional force can be accurately fitted to a general expression

$$f = -\eta(v/v_{\text{ref}})^k, \quad (1)$$

where v_{ref} is a reference velocity (set to 1 m/s), η is the so-called viscous coefficient and k is a parameter. Thus, in the range of velocity explored here the friction force remains in between the Stokes' ($f \propto v$) and the Coulomb's ($f = \text{constant}$) limit. This means, that even in the superlubricant regime the bilayers are away from equilibrium, resulting in $k \leq 1$. [31] We notice that for the soft bilayer, f grows dramatically for $v > 550$ m/s, when also the slider internal temperature has a steep increase [see Fig. 2(b)], an effect not found for the other curves up to 800 m/s. We then decide to fit the $f(v)$ profile to Eq. (1) only up to a maximum velocity, $v_{\text{max}} \sim 550$ m/s, and the corresponding results are reported in Table I.

Let us concentrate first on the homo-bilayers. In general, we find that as the rigidity of the system increases, k approaches unity and the viscous coefficient reduces. In fact, $k = 0.9$ ($\eta = 0.14$) for the H-H bilayer, becoming 0.83 (1.02) and 0.82 (5.29), respectively for N-N and S-S. This behaviour is related to the ability of the slider to thermalise against the substrate, a feature that depends on the layer rigidity. In fact, from panels (b)-(d) of Fig. 2 one can see that at any given velocity the slider temperature is larger for the softer layer, with H-H showing temperatures rather close to 300 K (T of the substrate).

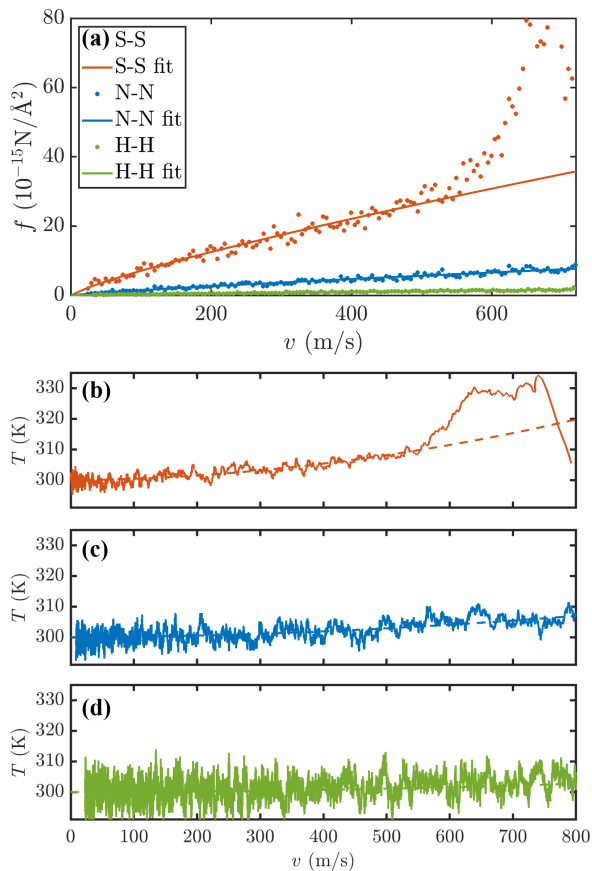


FIG. 2. (Color online) In the upper panel we present the friction force, f , as a function of the velocity for S-S, N-N and H-H MoS₂ homo-bilayers, where the circles are for the MD data and the lines are a fit to Eq. (1). In the lower three panels we show the slider temperature as a function of the velocity, again for (b) S-S, (c) N-N and (d) H-H. In these, the solid lines are from MD, while the dashed ones are calculated by mean field according to Eq. (3).

The elevated temperature of the slider indicates that the CM kinetic energy is efficiently converted into internal thermal energy, leading to friction.

As mentioned before the soft bilayer displays an anomalous high temperature for $v \gtrsim 550$ m/s, where the friction force abruptly deviates from Eq. (1); namely, as the slider is put in motion at 800 m/s, its internal temperature rapidly increases. This is because the friction is large and the vibration-energy flux injected into the slider exceeds the dissipative flux to the substrate. The latter is determined by the thermal coupling between the two layers. The elevated friction then causes a rapid reduction of the slider velocity, which in turn reduces the injected thermal flux. Thus, as the velocity drops, one reaches a steady-state situation in which the frictional energy injected is equal to the heat flow across the interface. Eq. (1) is then restored. A similar behaviour is found also for the N-N bilayer at $v \geq 1000$ m/s.

The low-velocity friction can be extrapolated from

TABLE I. Parameters fitting the $f(v)$ curve to Eq. (1). Here η is the viscous coefficient in 10^{-6} m·fs⁻¹s⁻¹ · ρ_s ($\rho_s = 18.84$ a.u./Å²), k is the velocity exponent and v_{\max} is the maximum velocity considered in the fit. The fit correlation factor is R , while G is the interfacial thermal conductance in units of MW/m²·K.

	η	k	ηk	v_{\max}	R	G
S-S	5.29	0.82	4.34	500	0.95	83.3
S-N	1.17	0.98	1.15	550	0.94	18.0
S-H	0.51	1.09	0.56	600	0.94	11.7
N-S	1.28	0.95	1.21	600	0.92	19.1
N-N	1.02	0.84	0.86	750	0.95	49.1
N-H	0.26	0.96	0.86	750	0.92	5.88
H-S	1.97	0.94	1.85	600	0.94	12.2
H-N	0.20	1.00	0.20	750	0.93	5.80
H-H	0.14	0.90	0.13	800	0.91	27.5

Eq. (1) by taking $f \propto \eta k v$, where the product ηk is effectively the Stokes' friction coefficient. These are also reported in Table I and clearly show a rather severe dependence of the low-velocity friction on the system rigidity. In fact, we find that doubling the stiffness leads to a friction reduction of approximately a factor six. Recalling that all the bilayers share an identical ISES, we conclude that the difference in friction is solely related to the layers internal dynamics and the thermal coupling between slider and substrate. Furthermore, by construction, all bilayers present an identical Γ -point breathing mode, which is associated to the rigid oscillation of the interlayer distance (see Fig. S1 in the supplemental material - SM). The kinetic energy associated to such mode, extracted from the vertical dynamics of the CM, does not change over the simulation time, meaning that it is not responsible for energy storing during the frictional motion. At the same time we observe little change in the interlayer distance, with the maximum increase of 0.015 Å found for S-S at $v > v_{\max}$. This, however, is consistent with the observed temperature profile and, therefore, it is not caused by scattering at the ISES.

Turning now our attention to heterostructures combining layers of different stiffness, Fig. 3 shows both the $f(v)$ and $T(v)$ profiles for all the possible six combinations. Starting from S-N and N-S, it is clear that the friction is independent from the layer order for $v < 500$ m/s, while above such velocity the soft slider is associated to a slightly larger friction. A more noticeable difference can be found in the T profile at high speed, where a soft slider moving on a normal substrate reaches 360 K, while a normal slider on a soft substrate does not exceed 330 K. More generally, the soft slider is constantly hotter than the normal one at any $v > 500$ m/s. Notably, in our classical MD simulations at high T monolayers of different stiffness have the same heat capacity. This means that the different $T(v)$ profile for S-N and N-S must be associated to a different heat flux, which develops despite the rather similar frictional forces in the two cases. Such variation in heat flux becomes negligible as the velocity

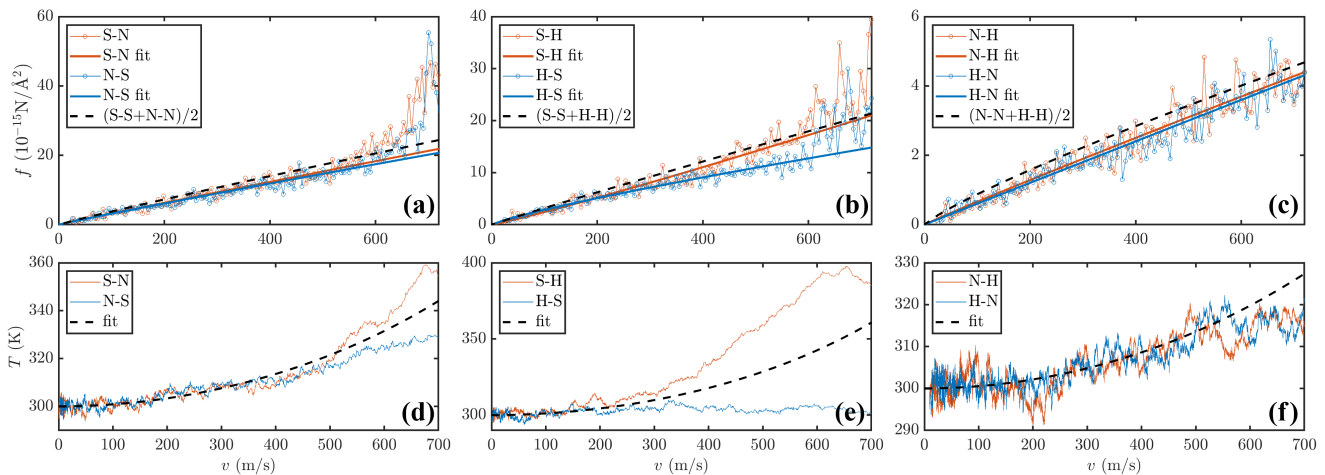


FIG. 3. Friction (upper panels) and slider temperature (lower panels) as a function of the slider velocity for the six different hetero-bilayers investigated. The MD data (thin lines and circles) are fitted to Eq. (1) (solid thick lines). The dashed lines in the friction plots are obtained by averaging the friction fitted to Eq. (1) for the corresponding homo-bilayers, while those in the temperature plots are calculated by using the prediction of Eq. (3).

is reduced below ~ 500 m/s.

From Fig. 3 we note that $f(v)$ computed for a hetero-bilayer is always smaller than the average friction of the associated homo-bilayers (dashed black lines), with the difference becoming more significant at high v 's. At the same time the temperature gap between the slider and the substrate (thermalised to 300 K) in hetero-bilayers is significantly larger than in homo-bilayers. These two facts together suggest that the thermal coupling between the layers in hetero-bilayers is weaker than in homo-bilayers. We can then model the friction as the sum of three contributions, $f = f_\alpha + f_\beta + f_{\alpha\beta}$, where f_α (f_β) is the friction originating from the energy dissipation to the slider (substrate) resulting from the ISES, while $f_{\alpha\beta}$ describes phonon-phonon scattering across the layers. Since the ISES is identical for all bilayers, f_α and f_β must remain unchanged with the bilayer composition at a give T . Hence, f of a hetero-bilayer remains lower than the average f of the associated homo-bilayers, because $f_{\alpha\beta}$ is smaller for hetero-bilayers. This feature originates from the reduced overlap between the phonon spectra of monolayers of different stiffness (Fig. S1 in SI).

An extreme situation is encountered for the S-H/H-S system [panels (b) and (e) of Fig. 3]. In this case the high-speed temperature increase is large for S-H (up to 400 K) and minimal for H-S, indicating that the main dissipation channel is through the soft layer. Since only the substrate is externally thermalised (as in vacuum experiments), such feature results in a two distinctly different $T(v)$ profiles, depending on the layers' order. By assuming f_{SH} and f_H to be much smaller than f_S , and by comparing the low- v $f(v)$ traces of the S-H and S-S systems, we can conclude that in the soft homo-bilayer f_{SS} contributes to about 30% of the total friction, namely it is similar to f_S over the entire v range. Finally, the N-H and H-N hetero-bilayers show similar friction and

temperature profiles, resembling the S-H case at low velocity. As the layers are both relatively rigid we do not note any significant heating at all velocities.

Our analysis can be made more quantitative by determining the interfacial thermal coupling between the layers. Since the out-of-plane thermal conductivity of a bilayer is ill-defined, we instead compute the interfacial thermal conductance, G . This simply relates the heat flux, q , with the temperature difference ΔT , $q = G\Delta T$, and it can be extracted from MD simulations. We first equilibrate the two layers at 400 K and 200 K, respectively. In the absence of external thermal reservoirs, the temperature difference between the two layers decays exponentially in time from its initial value, $\Delta T_0 = 200$ K (see Fig. 4), as

$$\Delta T(t) = \Delta T_0 \exp\left(-\frac{2G}{C_v}t\right), \quad (2)$$

where C_v is the specific heat. G can then be extracted by monitoring the time-evolution of ΔT . In performing the fit $C_v = 75.75$ J/mol·K $^{-1}$ is calculated from the total energy fluctuations. As expected G is found not to depend on the direction of the heat flux and the computed values (per unit area) are reported in Table I.

The thermal coupling between layers depends on the relative strengths of the inter- and intra-layer interactions, namely the binding energy and the bond stiffness. Thus, heat is transferred across the layers when the motion of the atoms in one layer drives the motion in the other. As the inter-layer van der Waals forces are identical for all heterostructures, in this case only the layer stiffness differentiates the thermal coupling. Thus, for homo-bilayers we find G to be relatively large and decreasing as the layer stiffness increases. In contrast, in hetero-bilayers, the interface conductance is determined

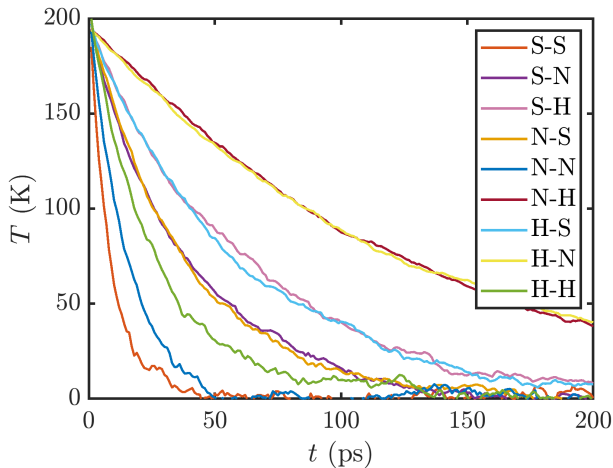


FIG. 4. (Color online) Time evolution of the temperature gap between the two layers of a bilayer, following equilibration at 400 K and 200 K, respectively. Each curve is the average over 10 different trajectories.

by the “acoustic mismatch”, namely by the relative thermal impedances, combined with the phonons coupling at the interface. These two factors together make the N-H combination being the less conductive and the S-N the most.

We are now in the position to complete our analysis. During the sliding process an heat flux, vf , is injected into the two layers. A steady-state situation is maintained when the heat transferred across the layers is constant and it is balanced by the heat flux to the thermostat in the substrate. In this situation we have

$$\Delta T = \frac{vf(v, T)}{2G}, \quad (3)$$

where $f \propto T^{1.6}$, a temperature dependence that has been obtained for the N-N bilayer by fitting Eq. (1) at different temperatures [see Fig. S2 in SM]. The calculated $T(v)$ profiles are then plotted in the panels (b)-(d) of Fig. 2

and (d)-(f) of Fig. 3 as dashed lines (when the substrate is thermostated then, $T(v) = \Delta T$). The curves show an excellent agreement between the measured temperature and that provided by Eq. (3), for both homo- and hetero-bilayers. This means that, for $v < v_{\max}$, there is steady-state heat flux across the layers, which is then broken at higher velocities, for which the severe heating of the slider is observed.

In summary, by using *ab-initio*-accurate force fields we have investigated the superlubricant state of MoS₂ bilayers. These have different in-plane stiffnesses, but identical inter-layer sliding energy surface, a feature that allows us to investigate the sole effect of the stiffness on the friction. In general, we find that the friction goes as v^k with the exponent remaining close to unity for rigid layers and deviating for soft layers and heterogeneous bilayers. For homo-bilayers a factor-two change in stiffness results in approximately a sixfold variation in friction. Hetero-bilayers follow a similar trend, although the low-velocity friction remains in general small. Similarly to other bilayer systems, we find that the out-of-plane motion of the layers is not a major energy dissipation channel.

The thermal coupling between the layers determines the heating during the sliding process. At low velocity a steady-state is established, where the temperature difference between the slider and the substrate sustains a constant heat flux. In this regime the friction and the temperature of the slider are independent on whether the slider is softer or harder than the substrate. In contrast, at elevated temperature the slider can heat up significantly, with the effect being much more pronounced for soft sliders. The crossover between these two regimes depends on the specific layer combinations. In particular, we find that hetero-bilayers composed of rigid materials can sustain ultra-low friction and moderate heat up even at extremely high velocities.

This work has been supported by IMRA Europe S.A.S. and by Science Foundation Ireland (grant 12/RC/2278_P2). We thank Stéphane Bourdais for discussion. Computational resources have been provided by the Trinity Centre for High Performance Computing (TCHPC).

-
- [1] M. Hirano and K. Shinjo, *Wear* **168**, 121 (1993).
 - [2] M.H. Müser, *Europhys. Lett.* **66**, 97 (2004).
 - [3] J.A. Van Den Ende, A.S. De Wijn and A. Fasolino, *J. Phys.: Condens. Matter* **24**, 445009 (2012).
 - [4] J.M. Martin, C. Donnet, Th. Le Mogne and Th. Epicier *Phys. Rev. B* **48**, 10583(R) (1993).
 - [5] L. Rapoport, Yu. Bilik, Y. Feldman, M. Homyonfer, S.R. Cohen and R. Tenne, *Nature* **387**, 791 (1997).
 - [6] M. Dienwiebel, G.S. Verhoeven, N. Pradeep, J.W.M. Frenken, J.A. Heimberg and H.W. Zandbergen, *Phys. Rev. Lett.* **92**, 126101 (2004).
 - [7] Z. Liu, J. Yang, F. Grey, J. Zhe Liu, Y. Liu, Y. Wang, Y. Yang, Y. Cheng and Q. Zheng, *Phys. Rev. Lett.* **108**, 205503 (2012).
 - [8] J. Yang, Z. Liu, F. Grey, Z. Xu, X. Li, Y. Liu, M. Urbakh, Y. Cheng and Q. Zheng, *Phys. Rev. Lett.* **110**, 255504 (2013).
 - [9] E. Koren, E. Lörtscher, C. Rawlings, A.W. Knoll and U. Duerig, *Science* **348**, 679 (2015).
 - [10] C. Qu, K. Wang, J. Wang, Y. Gongyang, R.W. Carpick, M. Urbakh and Q. Zheng, *Phys. Rev. Lett.* **125**, 126102 (2020).
 - [11] H. Li, J. Wang, S. Gao, Q. Chen, L. Peng, K. Liu and X. Wei, *Adv. Mat.* **29**, 1701474 (2017).
 - [12] O. Acikgoz and M.Z. Baykara, *Appl. Phys. Lett.* **116**, 071603 (2020).
 - [13] M.R. Vazirisereshk, K. Hasz, R.W. Carpick and A. Martini, *J. Phys. Chem. Lett.* **11**, 6900 (2020).

- [14] Y. Song, D. Mandelli, O. Hod, M. Urbakh, M. Ma and Q. Zheng, *Nature Mater.* **17**, 894 (2018).
- [15] H. Büch, A. Rossi, S. Forti, D. Convertino, V. Tozzini and C. Coletti, *Nano Res.* **11**, 5946 (2018).
- [16] J. Tian, X. Yin, J. Li, W. Qi, P. Huang, X. Chen and J. Luo, *ACS Appl. Mater. Interfaces* **12**, 4031 (2020).
- [17] A. Vanossi, N. Manini, M. Urbakh, S. Zapperi and E. Tosatti, *Rev. Mod. Phys.* **85**, 529 (2013).
- [18] E. Koren and U. Duerig, *Phys. Rev. B* **94**, 045401 (2016).
- [19] O. Hod, *ChemPhysChem* **14**, 2376 (2013).
- [20] A.S. De Wijn, A. Fasolino, A.E. Filippov and M. Urbakh, *Eur. Phys. Lett.* **95**, 66002 (2011).
- [21] I. Leven, D. Krepel, O. Shemesh and O. Hod, *J. Phys. Chem. Lett.* **4**, 115 (2013).
- [22] M. Reguzzoni, A. Fasolino, E. Molinari and M.C. Righi, *J. Phys. Chem. C* **116**, 21104 (2012).
- [23] X. Gao, W. Ouyang, O. Hod and M. Urbakh, *Phys. Rev. B* **103**, 045418 (2021).
- [24] W. Ouyang, M. Ma, Q. Zheng and M. Urbakh, *Nano Lett.* **16**, 1878 (2016).
- [25] Z. Wei, Z. Duan, Y. Kan, Y. Zhang and Y. Chen, *J. Appl. Phys.* **127**, 015105 (2020).
- [26] Y. Dong, Y. Tao, R. Feng, Y. Zhang, Z. Duan and H. Cui, *Nanotechnology* **31**, 285711 (2020).
- [27] A.P. Thompson, L.P. Swiler, C.R. Trott, S.M. Foiles and G.J. Tucker, *J. Comput. Phys.* **285**, 316 (2015).
- [28] A. Lunghi and S. Sanvito, *Science Adv.* **5**, eaaw2210 (2019).
- [29] A. Tkatchenko and M. Scheffler, *Phys. Rev. Lett.* **102**, 073005 (2009).
- [30] R. Dong, A. Jacob, S. Bourdais and S. Sanvito, *npj 2D Mater. Appl.* **5**, 26 (2021).
- [31] M.H. Müser, *Phys. Rev. B* **84**, 125419 (2011).